Citation: CPT Pharmacometrics Syst. Pharmacol. (2020) 9, 342–352; doi:10.1002/psp4.12518

ARTICLE

Leveraging Quantitative Systems Pharmacology Approach into Development of Human Recombinant Follistatin Fusion Protein for Duchenne Muscular Dystrophy

Hoa Q. Nguyen[1,5,*,†], Andrea Iskenderian[1,†], David Ehmann[1,†], Paul Jasper[2], Zhiwei Zhang[2], Haojing Rong[3], Devin Welty[4] and Rangaraj Narayanan[1,†]

Quantitative understanding about the dynamics of drug–target interactions in biological systems is essential, especially in rare disease programs with small patient populations. Follistatin, by antagonism of myostatin and activin, which are negative regulators of skeletal muscle and inflammatory response, is a promising therapeutic target for Duchenne Muscular Dystrophy. In this study, we constructed a quantitative systems pharmacology model for FS-EEE-Fc, a follistatin recombinant protein to investigate its efficacy from dual target binding, and, subsequently, to project its human efficacious dose. Based on model simulations, with an assumed efficacy threshold of 7–10% muscle volume increase, 3–5 mg/kg weekly dosing of FS-EEE-Fc is predicted to achieve meaningful clinical outcome. In conclusion, the study demonstrated an application of mechanism driven approach at early stage of a rare disease drug development to support lead compound optimization, enable human dose, pharmacokinetics, and efficacy predictions.

Study Highlights

WHAT IS THE CURRENT KNOWLEDGE ON THE TOPIC?
☑ To date, investigational drugs for Duchenne muscular dystrophy (DMD) have failed qualified success. Follistatin is a natural binding protein antagonist of myostatin and activin, which are suppressors of muscle growth and inducers of fibrosis. Follistatin has shown to promote generation of muscle tissues and inhibit activity of muscle suppressors, including myostatin and activin.

WHAT QUESTION DID THIS STUDY ADDRESS?
☑ This study examined an application of quantitative systems pharmacology (QSP) modeling to support the development of FS-EEE-Fc, an engineered recombinant protein, and assist discovery team with questions regarding to whether dual targets could lead to improved efficacy, how tight of binding of the drug to the receptor is needed, and, ultimately, what is the efficacious dose in humans.

WHAT DOES THIS STUDY ADD TO OUR KNOWLEDGE?
☑ This study presented the first QSP model for DMD, which mechanistically connects follistatin target engagement to muscle volume changes. The model suggested that dual pathway inhibition of activin and myostatin is expected to enhance muscle growth via activin receptor type IIB signaling.

HOW MIGHT THIS CHANGE DRUG DISCOVERY, DEVELOPMENT, AND/OR THERAPEUTICS?
☑ The presented QSP framework has potential to leverage known biological information of myostatin signaling pathway and incorporate recent clinical findings to support the ongoing clinical-stage drug programs as well as new strategies for targeting myostatin and its family members.

Duchenne muscular dystrophy (DMD) is a rare, fatal, neuromuscular disease, characterized by progressive skeletal muscle wasting and weakness; leading to loss of ambulation and premature death from respiratory and cardiac failure. DMD is caused by mutations in the gene encoding dystrophin, a critical structural protein of skeletal, cardiac, and smooth muscle. Currently, there are only a few approved drugs for patients with DMD, and they have limited efficacy.[1] Among different ongoing therapeutic strategies developed for DMD, including exon targets, micro-dystrophin, monoclonal antibodies against activin type 2 receptors, myostatin (also known as growth and differentiation factor-8) remains one of the popular drug targets.[2]

Several antagonists of myostatin have shown promise for enhancing muscle mass and strength in preclinical studies. One of the most potent of these agents, follistatin,

†A member of the Takeda group companies.
[1]Shire HGT, Inc. (a Takeda company), Lexington, Massachusetts, USA; [2]RES Group, Inc., Needham, Massachusetts, USA; [3]Kymera Therapeutics, Cambridge, Massachusetts, USA; [4]Nuventra Pharma Sciences, Research Triangle Park, North Carolina, USA; [5]Present address: Takeda Pharmaceuticals International Co, Cambridge, Massachusetts, USA. *Correspondence: Hoa Q. Nguyen (hoa.nguyen@takeda.com)
Received: January 7, 2020; accepted: April 13, 2020. doi:10.1002/psp4.12518

an endogenous circulating glycoprotein, can prevent myostatin from binding to activin type IIB receptor (ActRIIB) on muscle cells, leading to muscle-enhancing effects. Transgenic mouse studies have shown that myostatin is not the sole regulator of muscle mass and follistatin can promote muscle growth by blocking not only myostatin but also other ligands with similar activity to myostatin.[3] This hypothesis was verified by our recent studies using FS-EEE-Fc, an engineered recombinant protein, designed to bind to myostatin and activin A, block their activities, and promote muscle growth.[4,5] The FS-EEE-Fc molecular structure, which comprises of circulating long form of follistatin and a linker to the Fc region of human immunoglobulin IgG1, was optimized with reduced heparin binding to improve pharmacokinetic (PK) properties.[5] *In vitro* binding, PK properties and pharmacological effects of FS-EEE-Fc were described in previous publications.[4,5] Based on the effects of follistatin on inflammation and fibrosis, in addition to increasing muscle mass and strength, delivery of FS-EEE-Fc is potentially useful for treating patients with DMD.

During development of FS-EEE-Fc, there is a need for a quantitative framework to demonstrate the promise of FS-EEE-Fc biology with dual target binding and provide an informed human efficacious dose projection. Although having their own advantages, conventional PK/pharmacodynamic (PD) models typically lack detailed mechanistic descriptions of the dynamics of interactions between drug and biological system. Aiming to differentiate the potential efficacy of FS-EEE-Fc and understand the behavior of the system as whole, a quantitative systems pharmacology (QSP) approach was applied in this study. In addition, difficulties in developing therapies for DMD arise from the small patient population (mainly boys 4–18 years old), complex nature of the disease, and challenges in identifying relevant biomarkers and clinical endpoints. Therefore, we used a QSP approach with attempts to integrate limited data, fill the knowledge gaps, and support knowledge-building in muscular dystrophy disease.

In this work, disposition and interactions between FS-EEE-Fc with myostatin and activin A were illustrated in a biological process map (**Figure 1**) based on available knowledge of DMD disease biology, myostatin and activin kinetics, and FS-EEE-Fc biochemical/PK properties. Myostatin is predominantly expressed in skeletal muscle and plays a pivotal role in regulating skeletal muscle mass and function.[6–8] The molecular mechanism of the myostatin signaling pathway has been recently reviewed,[9,10] in which myostatin regulates muscle by signaling through activin receptors and downstream Smad transcription factors. The downstream effect of myostatin binding to its high affinity receptor, ActRIIB, ultimately gives rise to muscle wasting.[9] Activin A, a member of the transforming growth factor beta superfamily, is well-characterized with its role in modulating follicle-stimulating hormone (FSH) release from the pituitary. Activin A is a critical mediator of inflammation and immunity, and was measured at elevated levels in circulation in a wide range of pathological conditions.[11] Additionally, besides myostatin, activin A was found to be a second key player in the regulation of muscle growth.[12–15]

Myostatin inhibitors have been in clinical trials for more than a decade. Among those include ACE-031 (soluble decoy receptor), bimagrumab (monoclonal antibody (mAb) against ActRII receptors), anti-myostatin mAb PF-06252616 (domagrozumab), and the anti-myostatin adnectin BMS-986089/RO7239361 programs. With recent termination of domagrozumab, BMS-986089 and ACE-083 trials due to lack of efficacy, so far, no agent has yet translated muscle hypertrophy in preclinical to measurable improvements in patient strength and function. Different from these molecules targeting myostatin alone, FS-EEE-Fc was developed to boost regeneration of muscle tissue and prevent progression of fibrosis by binding to multiple targets of myostatin and activin A.

On these bases, the objectives of this work were: (i) to develop a QSP model integrating FS-EEE-Fc disposition characteristics, modulation of key biological components, and dynamic interactions between the drug and targets leading to muscle volume changes; (ii) to evaluate its predictive capacity in recapitulating the extent of muscle growth from different myostatin inhibitors in humans; and (iii) to demonstrate its applicability in selecting an optimal drug candidate and projecting human efficacious dose for FS-EEE-Fc.

METHODS

Data sources for model development

Data were collected from different sources for model development and qualification, including relevant physiological parameters, clinical data of myostatin inhibitors published in literature, and *in vitro/in vivo* experimental studies of FS-EEE-Fc.

Clinical data of myostatin inhibitors. Several myostatin inhibitors have been developed and progressed into clinical development for muscular disorders.[2,10] Clinical data of anti-myostatin adnectin (BMS-986089),[16] ACE-031,[17] and domagrozumab (PF-06252616)[18] was used for human model calibration and qualification. PK and muscle volume observations from these publications were digitized using WebPlotDigitizer version 4.1 (https://apps.automeris.io/wpd/).

Experimental data of FS-EEE-Fc. Preclinical data of FS-EEE-Fc was used to calibrate the QSP model for FS-EEE-Fc in animal species. Pharmacology of FS-EEE-Fc was studied in mice to illustrate the effect of FS-EEE-Fc on body weight and muscle mass. Regarding activin inhibition, an ovariectomized rat study was conducted to evaluate downstream effect of FS-EEE-Fc on FSH level through activin binding. Monkey PK data were used to estimate PK parameters, which were subsequently scaled to project the human PK profile of FS-EEE-Fc. Details of experimental studies are provided in the **Supplementary Methods**.

DMD QSP model development

Modeling strategy. Overall, the schematic strategy for model development is shown in **Figure S1**. To support model development, data comes from clinical and preclinical sources. A human model for myostatin inhibitors, including adnectin (BMS-986089), anti-myostatin mAb (domagrozumab), and ActRIIB soluble protein (ACE-031), was built using reported physiological parameters, compound

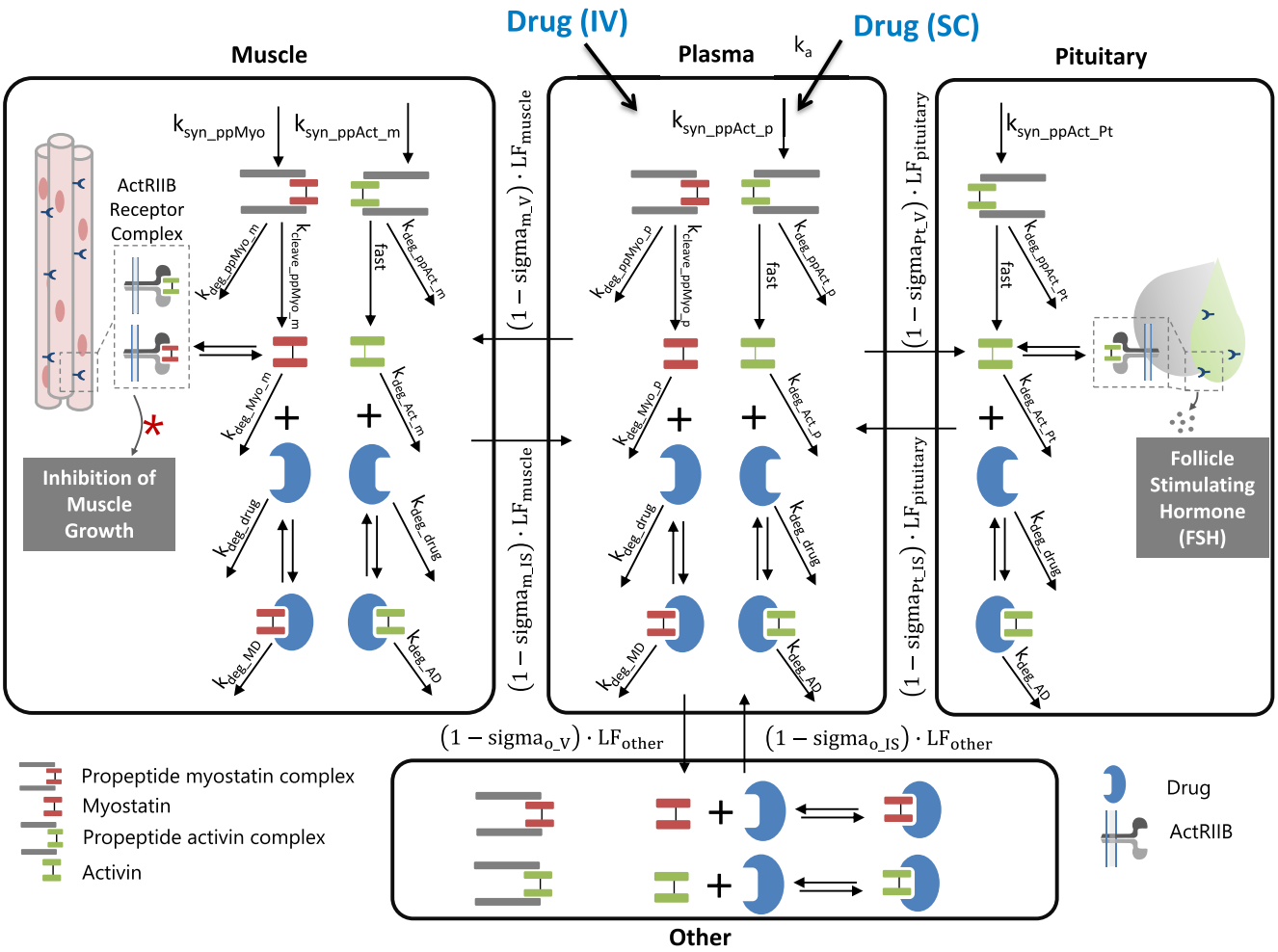

Figure 1 Structure of quantitative systems pharmacology model for FS-EEE-Fc and other myostatin/activin inhibitors. Disposition of the drug and different molecular entities was described in relevant physiological compartments, including muscle, pituitary, plasma, and other organ tissues. In the molecular level of model, myostatin and activin interact with activin type IIB receptor (ActRIIB), leading to inhibition of muscle growth. Myostatin and activin also bind to FS-EEE-Fc or other myostatin/activin inhibitors that act as ligand traps to block the interaction of these ligands with ActRIIB.

specific parameters, and published clinical data. In this model, muscle growth was driven by the magnitude of ActRIIB receptor occupancy (RO), and PD parameters were obtained by fitting the model to adnectin data. In parallel, a model for FS-EEE-Fc was developed for the mouse, rat, and monkey using FS-EEE-Fc preclinical data and translated to humans using corresponding physiological parameters and allometric scaling. Coupled with the established ActRIIB RO and muscle growth correlation, a final human model for FS-EEE-Fc was executed to predict the human efficacious dose and efficacy.

The model was mathematically presented by a set of ordinary differential equations described in **Supplementary Information**. The mathematical model was implemented in R version 3.5.0. (deSolve, FME,[19] and R Shiny) for simulation and Matlab Simbiology R2019a for optimization.

Structure of DMD QSP model. A QSP model for myostatin/activin inhibitors including FS-EEE-Fc and other clinical candidates in DMD was constructed and its diagram was shown in **Figure 1**, illustrating the disposition of the drug and different molecular entities in relevant physiological compartments, namely the muscle, pituitary, plasma, and other tissues. To establish DMD disease biology in quantitative framework, a systems pharmacology approach was adopted. The biological process map (**Figure 1**) incorporates key features related to myostatin and activin kinetics, such as (i) synthesis and cleavage of latent complexes to release active or mature myostatin and activin, (ii) distribution of myostatin and activin related species in plasma and interstitial compartments, and (iii) myostatin and activin binding to ActRIIB receptors leads to inhibition of muscle growth and FSH secretion. Details of the model description are presented in **Supplementary Methods**.

Model parameterization. The human model parameters' values, their sources, and assumptions for myostatin, activin, FS-EEE-Fc, and other myostatin inhibitors were tabulated in **Tables 1** and **2**. In general, physiological parameters, including plasma, muscle and pituitary interstitial volumes, and lymph flows, were obtained or estimated from literature

Table 1 System parameters of myostatin and activin in humans

Model parameters			Unit	Definition	Value	Source note
System		V_{plasma}	L	Volume of plasma	3.126	Shah, 2012[25]
		V_{muscle}	L	Interstitial volume of muscle	3.91	Shah, 2012[25]
		$V_{pituitary}$	L	Interstitial volume of pituitary	5.4×10^{-5}	Calculated based on Lit
		LF_{muscle}	L/hour	Lymph flow of muscle	0.335	Shah, 2012[25]
		$LF_{pituitary}$	L/hour	Lymph flow of pituitary	1.34×10^{-6}	Calculated based on Lit
		LF_{other}	L/hour	Lymph flow of other tissues	0.297	Calculated based on Lit
	Myostatin	MW_{Myo}	g/mol	MW of Myo	25,000	Thies *et al*., 2000[36]
		MW_{ppMyo}	g/mol	MW of ppMyo	80,000	Thies *et al*., 2000[36]
		k_{syn_ppMyo}	1/hour	Synthesis rate of ppMyo	0.809	Calibrated
		$k_{cleave\_ppMyo\_m}$	1/hour	Cleavage rate of ppMyo in muscle	0.0698	Calibrated
		$k_{cleave\_ppMyo\_p}$	1/hour	Cleavage rate of ppMyo in plasma	0.01	Calibrated
		$k_{deg\_ppMyo\_m}$ (OR _p, _o)	1/hour	Degradation rate of ppMyo in muscle (or pituitary, other tissues)	0.346	Wakefield, 1990[37]
		$k_{deg\_Myo\_m}$ (OR _p, _o)	1/hour	Degradation rate of Myo in muscle (or pituitary, other tissues)	0.346	Wakefield, 1990[37]
		$sigma_{m\_V\_ppMyo}$ (OR _myo)	dimensionless	Vascular reflection coefficient for muscle of ppMyo (or Myo)[a]	0.7	Li, 2019[29]
		$sigma_{m\_IS\_ppMyo}$ (OR _myo)	dimensionless	Lymphatic reflection coefficient for muscle of ppMyo (or Myo)[a]	0.2	Shah, 2012[25]
		$kon_{Myo\_ActRIIB}$	1/(nM.hour)	Association rate constant of myostatin-receptor binding	1.328	Sako, 2010[38]
		$koff_{Myo\_ActRIIB}$	1/hour	Dissociation rate constant of myostatin-receptor complex	0.124	Sako, 2010[38]
	Activin	MW_{Act}	g/mol	MW of activin	25,000	Literature
		MW_{ppAct}	g/mol	MW of ppAct	80,000	Literature
		$k_{syn\_ppAct\_Pt}$	1/hour	Synthesis rate of ppAct in pituitary	9.1×10^{-6}	Calibrated
		$k_{syn\_ppAct\_p}$	1/hour	Synthesis rate of ppAct in plasma	0.12	Calibrated
		$k_{syn\_ppAct\_m}$	1/hour	Synthesis rate of ppAct in muscle	0.0698	Calibrated
		k_{cleave_ppAct}	1/hour	Cleavage rate of ppAct	3,113	Calibrated
		$k_{cleave\_ppAct\_p}$	1/hour	Cleavage rate of ppAct in plasma	3,113	Calibrated
		$k_{deg\_ppAct\_Pt}$ (OR _p, _m, _o)	1/hour	Degradation rate of ppAct in pituitary (or plasma, muscle, or others)	1.386	Johnson, 2016[39]
		$k_{deg\_Act\_Pt}$ (OR _p, _m, _o)	1/hour	Degradation rate of Act in pituitary (or plasma, muscle, or others)	2.08	Johnson, 2016[39]
		$sigma_{m\_V\_ppAct}$ (OR _Act)	dimensionless	Vascular reflection coefficient for muscle of ppAct (or Act)[b]	0.7	Li, 2019[29]
		$sigma_{m\_IS\_ppAct}$ (OR _Act)	dimensionless	Lymphatic reflection coefficient for muscle of ppAct (or Act)[b]	0.2	Shah, 2012[25]
		$kon_{Act\_ActRIIB}$	1/(nM.hour)	Association rate constant of activin-receptor binding	14.90	Sako, 2010[38]
		$koff_{Act\_ActRIIB}$	1/hour	Dissociation rate constant of activin-receptor complex	0.533	Sako, 2010[38]
	ActRIIB	ActRIIB Concentration	nM	ActRIIB receptor concentration in muscle or pituitary compartment	0.138	Calculated based on Lit

Act, activin; ActRIIB, activin type IIB receptor; MW, molecular weight; Myo, myostatin; ppAct, activin propeptide complex; ppMyo, myostatin propeptide complex.
[a]Similar values of ppMyo or myostatin vascular and lymphatic coefficients were assumed for other tissues. [b]Similar values of ppAct or activin vascular and lymphatic coefficients were assumed for pituitary and other tissues.

as described in **Supplementary Methods**. System parameters regarding myostatin and activin kinetics, such as synthesis, cleavage, and degradation rates, were fine-tuned to recapitulate the steady-state levels of these ligands in plasma and tissues of interest. Human PK parameters of FS-EEE-Fc were projected from monkey PK parameters (**Table S3** in **Supplementary Tables**) using simple allometry for V_{other} with scaling exponent of 1.12 for soluble ligands.[20] Human PD parameters of follistatin were obtained by fitting the model to clinical data of other myostatin inhibitors. For other drug candidates, compound-specific parameters were estimated via global optimization based on their sensitivity analyses (SAs; **Supplementary Methods**).

The optimization toolbox with *fminsearch* and *particle swarm* algorithm in MatLab Simbiology was used for parameter estimation. Based on local and global SA (**Supplementary Methods**), sensitive parameters were estimated by simultaneously fitting the model to drug and myostatin (when

Table 2 Compound-specific parameters of FS-EEE-Fc and other myostatin inhibitors in humans

Model parameters		Unit	Definition	Human value				Source note
				FS-EEE-Fc	Adnectin	ACE-031	Domagro-zumab	
Compound-specific	MW_{Drug}	g/mol	MW of drug	150,000	76,000	100,000	150,000	Literature
	V_{subcu}	L	Volume of subcutaneous space	0.01	0.01	0.01	0.01	Assumed
	F	dimensionless	Bioavailability	0.7[a]	0.7[b]	0.7[b]	0.75[c]	Preclinical data, literature
	k_a	1/hour	Absorption rate	0.027[a]	0.029	0.011	-	Human PK data
	V_{other}	L	Volume of other tissues	8.28[a]	10.3	0.38	3.36	Human PK data
	k_{deg_drug}	1/hour	Degradation rate of drug	0.008[a]	0.0016	0.0019	0.0014	Human PK data
	$kon_{drug\text{-}Myo}$	1/(nM.hour)	Association rate constant of drug-Myo binding	0.6	0.22	0.6	0.389	Human PK data
	$koff_{drug\text{-}Myo}$	1/hour	Dissociation rate constant of drug-Myo complex	0.0045[d]	0.013	0.0561[e]	0.00153	Human PK data, *in vitro* Kd
	$sigma_{m\_V\_drug}$	dimensionless	Drug vascular reflection coef. for muscle[h]	0.98[f]	0.72	0.80	0.98	Human PK data
	$sigma_{m\_IS\_drug}$	dimensionless	Drug lymphatic reflection coef. for muscle[h]	0.2	0.2	0.2	0.2	Shah, 2012[25]; Li, 2019[29]
	k_{deg_MD}	1/hour	Degradation rate of drug-Myo complex	0.006	0.0016	0.0019	0.0014	Assumed ~ k_{deg_drug}
	k_{deg_AD}	1/hour	Degradation rate of drug-Act complex	0.006	0.0016	0.0019	0.0014	Assumed ~ k_{deg_drug}
	$kon_{drug\text{-}Act}$	1/(nM.hour)	Association rate constant of drug-Act binding	0.6[i]	0.6[i]	0.6[i]	0.6[i]	Assumed
	$koff_{drug\text{-}Act}$	1/hour	Dissociation rate constant of drug-Act complex	0.0037[d]	6×10^{5}[g]	0.0214[e]	6×10^{5}[g]	Calculated from *in vitro* Kd
	V_{max_muscle}	Dimensionless	Maximal muscle increase	0.005				Human muscle volume data
	h_{muscle}	Dimensionless	Hill coefficient of muscle	6				Human muscle volume data
	RO_{50_muscle}	%	%RO that lead to 50% muscle increase	23.36				Human muscle volume data
	k_{deg_muscle}	1/hour	Degradation rate of muscle	0.0002				Human muscle volume data
	V_{max_FSH}	ng/mL/hour	Maximal FSH	25.75				Human FSH data
	h_{FSH}	Dimensionless	Hill coefficient of FSH	1.80				Human FSH data
	RO_{50_FSH}	%	%RO leads to 50% FSH decrease	21.78				Human FSH data
	k_{deg_FSH}	1/hour	Degradation rate of FSH	1.00				Human FSH data

%RO, percentage of receptor occupancy; coef., coefficient; FSH, follicle-stimulating hormone; MW, molecular weight; Myo, myostatin; PK, pharmacokinetic. [a]Value obtained from allometric scaling using monkey data. [b]Value was set as typical s.c. bioavailability for therapeutic proteins.[40] [c]Value obtained from Bhattacharya *et al*. (2018).[41] [d]Value estimated from published Kd of 7.5 and 6.1 pM[4]. [e]Value estimated from published Kd in Sako *et al*.[38] [f]Vascular reflection coefficient of FS-EEE-Fc in humans was assumed to be similar to the value of Domagrozumab with the same MW. [g]Arbitrary high value to assume negligible binding to activin. [h]Similar values of drug vascular and lymphatic coefficients were assumed for pituitary and other tissues. [i]Value was set as a typical association rate (k_{on}) of monoclonal antibodies.[42]

available) serum concentration-time profiles from different doses. Final estimated PK parameters were then fixed for anti-myostatin adnectin and ACE-031 to subsequently calibrate the QSP model to muscle volume increase and FSH levels using adnectin and ACE-031 clinical PD data, respectively. The fit was evaluated based on visual inspection, observed vs. predicted plots, predicted vs. residual plots and percentage of coefficient of variation of the final estimates.

Model evaluation

To evaluate the predictive capability of the QSP model for muscle volume increase, we used the model to simulate muscle volume changes for ACE-031 and domagrozumab, which were not used in the model calibration step. The simulated values were then compared with observed muscle volume increase by these compounds in clinical studies.

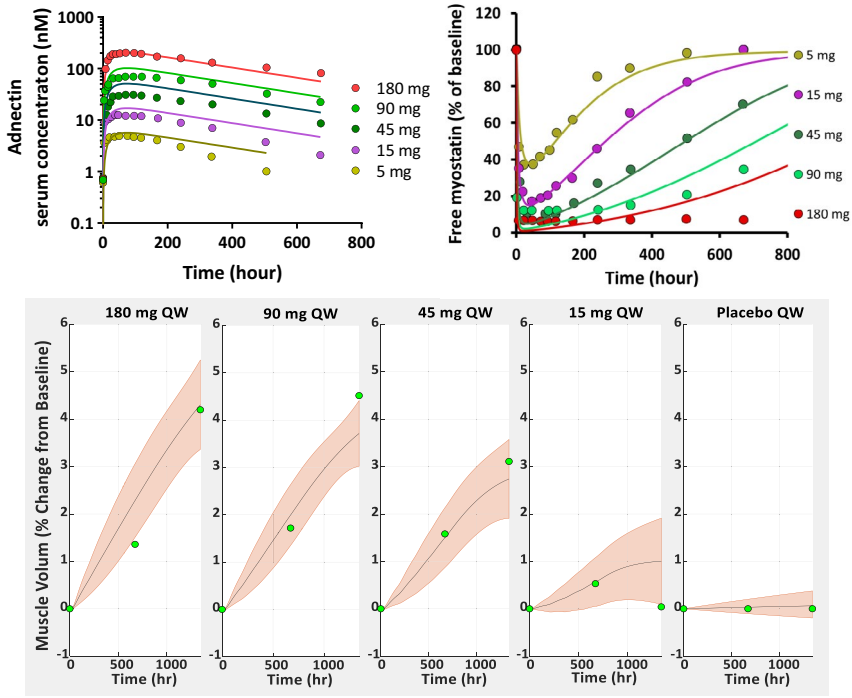

Figure 2 Model calibrations to clinical pharmacokinetic (upper panel) and muscle growth data (lower panel) of anti-myostatin adnectin. Data points represent clinical observations that were used for parameter estimation. Lines represent fitted curves and 95% confidence interval for the model predictions that were generated using the estimated parameters by Gaussian method. With fit results obtained from parameter estimation, the function in MatLab computes the Gaussian confidence intervals for each estimated model response at every time step.

RESULTS

Development of a core QSP model for myostatin inhibitors

Establish myostatin and activin kinetics and corresponding contributions to ActRIIB receptor occupancy at steady-state. System parameters regarding myostatin/activin homeostasis levels are listed in **Table S1**. Based on these reported values, model parameters related to ligand kinetics were fine-tuned to capture the levels of these components in plasma, muscle, and pituitary. Final estimates of synthesis, cleavage, and degradation rates are presented in **Table 1**. **Table S2** listed the simulated ActRIIB receptor occupancies contributed by myostatin and activin in muscle tissues for different species. In humans, at steady-state, myostatin and activin can bind up to 50% of ActRIIB receptors. Meanwhile, due to their higher baseline levels in rodents, myostatin and activin can occupy up to 70–90% total ActRIIB RO in rats and mice.

Parameter sensitivity analysis. Local SA was performed to identify parameter(s) with the highest impact on the model outcome. **Figure S2** (**Supplementary Figures**) presented most important parameters on the concentration-time profile of the drug, including V_{other}, $k_{deg\text{-}drug}$, k_a, and $sigma_{m\_V\_drug}$. Sensitivity analyses indicate that the vascular coefficient is indeed an important parameter governing serum adnectin concentrations. In addition to these parameters, drug binding affinity was found to have significant impact on the prediction of myostatin disposition. Extent of muscle volume increase is sensitive to the accuracy of V_{max_muscle}, $RO_{50\text{-}muscle}$, and h_{muscle} parameters. The $k_{deg\text{-}muscle}$ seems to have little effect on the model prediction of muscle growth. In global SA, based on the scatterplots (**Figure S3**), correlations between outputs vs. parameter values indicate that $k_{deg\text{-}drug}$, $sigma_{m\_V\_drug}$, V_{other}, $kon_{drug\text{-}Myo}$, $koff_{drug\text{-}Myo}$, V_{max_muscle}, $RO_{50\text{-}muscle}$, and h_{muscle} are the most critical parameters that influence drug area under the curve (AUC), myostatin AUC, and muscle growth predictions. The rate of absorption turns out less sensitive in global SAs, which can be explained for therapeutic protein with long half-life, eventually k_a is less important to the overall drug exposure. In local SAs, the model outcome consisted of each data point in the drug concentration-time profile, whereas in global SAs, the model output was the overall AUC of drug disposition. With this difference, overall, the global SAs resulted in similar conclusion as local SAs regarding the list of important parameters.

Calibrate muscle growth component of QSP model using clinical data of anti-myostatin adnectin. The human QSP model was fitted to anti-myostatin adnectin (BMS-986089) digitized data to obtain model parameters that characterize human muscle growth. **Table 1** tabulated fitted PK and PD parameters for anti-myostatin adnectin. Model predictions of drug, free myostatin serum concentrations, and muscle volume increase were overlaid with observed data, which are shown in **Figure 2**. Overall,

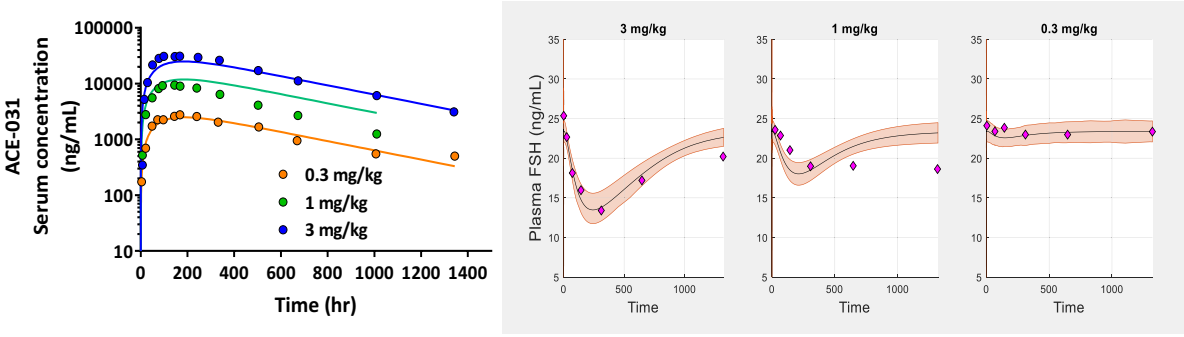

Figure 3 Model calibrations to clinical pharmacokinetic (left panel) and pharmacodynamic of follicle-stimulating hormone levels (right panel) of ACE-031. Data points represent clinical observations that were used for parameter estimation. Lines represent fitted curves and 95% confidence interval for the model predictions that were generated using the estimated parameters by Gaussian method. With fit results obtained from parameter estimation, the function in MatLab computes the Gaussian confidence intervals for each estimated model response at every time step.

the model was able to capture the disposition profile of anti-myostatin adnectin and its effect on muscle growth at a given dose. Free myostatin in plasma after adnectin single dose administration were also well described without recalibrating myostatin baseline kinetics. The good alignment suggests that model molecular parameters for myostatin, including its k_{syn}, k_{cleave}, and k_{deg} are acceptable. Muscle volume increase in four dose groups are spread within 95% confidence interval of model prediction. Based on the quality of the fit, empirical relationship, and estimated parameters between ActRIIB RO and muscle growth was deemed to be reasonable to link the drug exposure, ActRIIB RO, and muscle volume PD readout.

Calibrate the FSH reduction component of QSP model using ACE-031 clinical data. ACE-031 is a soluble fusion protein comprised of an extracellular domain of a form of activin receptor type IIb linked to Fc region of IgG1. The human QSP model was fitted to ACE-031 PK and PD data to obtain the PD parameters of FSH submodel as inputs for the FS-EEE-Fc model in humans (**Table 1**). Observed data, simulated mean, and 95% confidence interval of FSH plasma concentration are illustrated in **Figure 3**. In healthy postmenopausal women, the 43% decrease in serum FSH observed after a single dose of 3 mg/kg ACE-031 demonstrated a known biological effect of activin inhibition. As seen in **Figure 3**, the model decently describes the PK and PD effect of ACE-031 on FSH levels after 0.3 and 3 mg/kg doses.

Qualify the QSP model using clinical Domagrozumab and ACE-031 muscle volume increases. After benchmarking the model with ACE-031 PK data, without changing PD parameters of muscle growth obtained from the step above, the integrated QSP model was used to simulate muscle volume increase in healthy postmenopausal women and compare with observed data in Attie *et al.*[17] Similarly, domagrozumab muscle volume change was also used to test the predictive capability of the muscle growth submodel after domagrozumab PK calibration (**Figure S4**). The model forward-simulated and observed values of muscle volume changes in ACE-031 and domagrozumab studies are reported in **Table 3**.

Table 3 Simulated and observed muscle volume changes

		Muscle volume increase (%)	
Drug candidate	**Dose**	**Simulated**	**Observed**
ACE-031	1 mg/kg	2.0	3.5 ± 2.9[17]
	3 mg/kg	3.14	5.1 ± 4.2[17]
Domagrozumab	10 mg/kg	5.64	4.49[18]

Model applications to FS-EEE-Fc

The model was adapted to our drug candidate, FS-EEE-Fc, by adjusting corresponding system parameters for animals (**Tables S3 and S4**) and calibrating to PK/PD profiles from preclinical studies of FS-EEE-Fc, to demonstrate target engagement and dual target efficacy of FS-EEE-Fc in preclinical species.

Demonstrate FS-EEE-Fc target engagement. The preclinical model of FS-EEE-Fc was fitted to mouse serum profiles after a single i.v. dose of 1 mg/kg (**Figure S5**). Parameter estimates were reasonably precise and listed in **Table S4**. The model was then calibrated to muscle mass increase data to obtain muscle PD parameters of FS-EEE-Fc model in mice. As seen in **Figure S6A**, the empirical model of indirect response that relates the RO of ActRIIB to muscle growth was able to describe muscle growth data in *mdx* mice at different doses.

Similarly, the model was calibrated to OVX rat data to demonstrate the engagement of FS-EEE-Fc with activin, leading to the decrease of FSH in plasma due to effect of FS-EEE-Fc on FSH modulation. In **Figure S6B**, the experimental and simulated data illustrated evidence of this target engagement that, by increasing FS-EEE-Fc dose, the ActRIIB RO by activin would decrease, leading to significant decrease of FSH levels.

Demonstrate potential efficacy of dual target inhibition. Myostatin is recognized as the predominant negative regulator of muscle growth, likewise, activin was

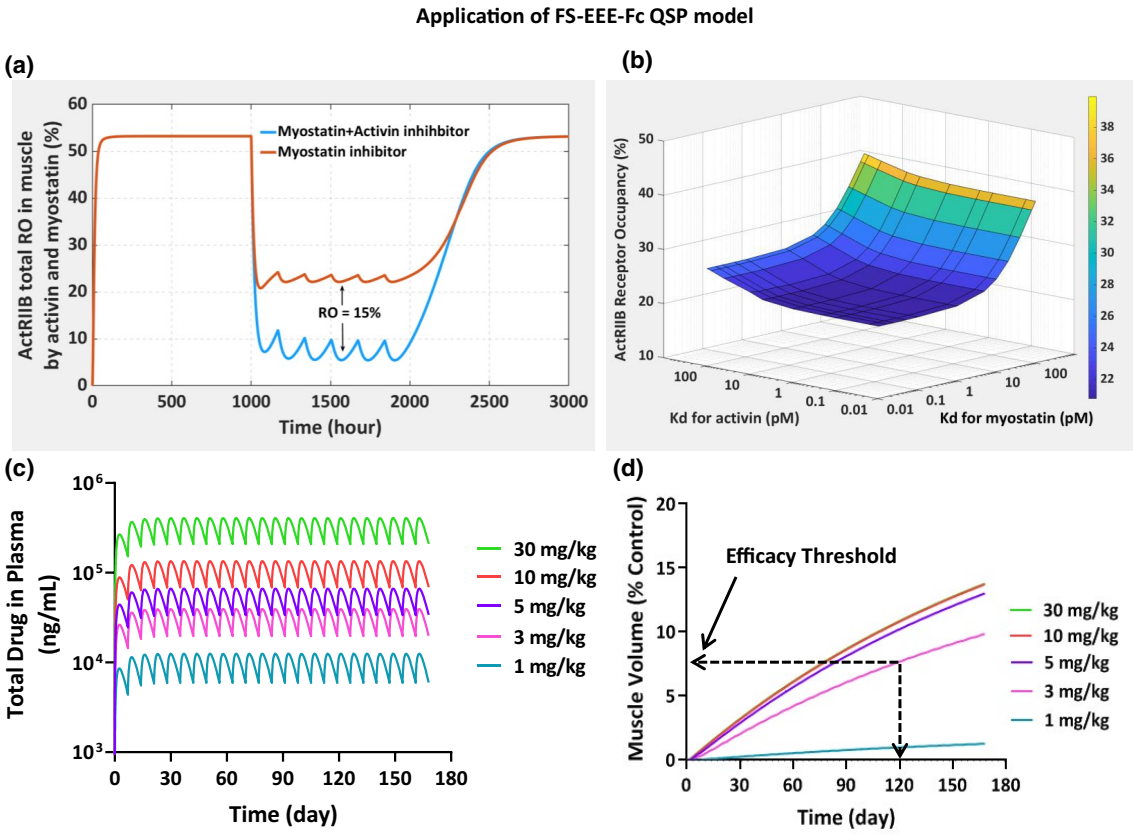

Figure 4 Model was applied for FS-EEE-Fc to demonstrate potential efficacy of dual target antagonist (**a**), to explore optimal binding affinities (**b**), and to project human pharmacokinetic (**c**), and efficacious dose (**d**).

found to be a second player in regulating muscle size and mass.[12] By including both activin and myostatin in a mechanistic model with their corresponding receptor occupancies, the model simulations (**Figure 4a**) showed that inhibiting activin and myostatin can reduce ActRIIB RO by additional 10% compared with only myostatin inhibition. The model suggested that dual pathway inhibition is expected to enhance muscle growth via ActRIIB signaling. The model simulation is in alignment with findings from a study in *mdx* mice suggesting that activin and myostatin inhibition synergistically increase muscle weight.[4]

Identify optimal myostatin/activin binding affinity balance

When being developed at an early stage, a mechanistic model can guide the design of lead candidates by identifying the optimal myostatin/activin binding affinity balance in a dual antagonist. In **Figure 4b**, for FS-EEE-Fc, at 3 mg/kg s.c., the model indicated that binding affinity to activin is less sensitive to total ActRIIB RO. At any value of myostatin K_d, changing the K_d for activin from 0.01 to 100 pM, the total ActRIIB RO would change ~ 4%. However, if changing myostatin K_d, the total RO may change from 20–40%. The current FS-EEE-Fc molecule binds tightly to both ligands at optimal K_d values of 7.5 and 6.1 pM. Decreasing these binding affinities by 100-fold would not change the total RO significantly.

Project human efficacious dose. Monkey PK characteristics were used to project human PK profile of FS-EEE-Fc. PK parameters were estimated by fitting the monkey QSP model to PK profiles of three dose groups simultaneously (**Figure S6**). The links between ActRIIB RO—muscle growth and between ActRIIB RO—FSH levels were described by the established correlations obtained above based on clinical data of other drug candidates.

Prior to simulating a human dose, a criteria/threshold of efficacy was assessed for clinical success. We conducted a thorough literature search of clinical trials of DMD drug candidates[16–18,21–24] to make an assumption that at least 7% muscle volume increase would potentially lead to significant clinical outcome of the 6-minute walk test (6MWT). Clinical end points of these myostatin inhibitors (BMS-986089, domagrozumab, ACE-031, and bimagrumab) were included in **Table S4**. Significant increases (4–7%) in thigh muscle volume were observed following administration of these agents in healthy volunteers after 1–3 months. In boys with DMD, data from phase I/II studies of BMS-986089 showed generally increasing trends in muscle volume at week 24 vs. placebo.[21] ACE-031 treatment led to change in total body lean mass of boys with DMD from

3.6–4.1% compared with baseline.[22] Bimagrumab was developed for treating inclusion-body myositis, a rare muscle wasting disease. In a phase II trial in sporadic inclusion body myositis, bimagrumab increased thigh muscle volume of 7.1% compared with placebo.[24] Even if bimagrumab or other drugs show that they can build significant muscle mass and strength, these drugs failed to meet their primary efficacy endpoint of the 6MWT or 4-stair climb in phase II/III studies. Taken together, we concluded that to achieve functional improvement for boys with DMD, inhibiting myostatin and getting 4–7% muscle growth is not adequate. At least 7% or above of muscle volume increase could potentially translate to significant clinical outcome.

With this predefined efficacy threshold, we ran model simulations for a range of FS-EEE-Fc doses from 1–30 mg/kg weekly s.c. dosing (**Figure 4c,d**). To achieve at least 7% muscle volume increase, a weekly i.v. or s.c. dose of 3–5 mg/kg FS-EEE-Fc is predicted for patients with DMD to result in meaningful clinical outcome. A Shiny app (https://hoaqnguyen.shinyapps.io/Anti-myostatinQSPmodel/) was created for illustration of QSP model predictions for FS-EEE-Fc in humans at different dose levels and number of doses.

DISCUSSION

In the absence of dystrophin, muscle degeneration and weakness cause loss of ambulation in patients with DMD. Therefore, minimizing muscle wasting and enhancing muscle mass/strength have been proposed as a promising treatment strategy for patients with DMD. FS-EEE-Fc is a follistatin recombinant protein that involves a complex interplay of multiple ligand engagement. The QSP model for FS-EEE-Fc can serve as an example of an useful translational tool to support a discovery team's decisions. At the early stage of drug development, this model can help to navigate through some key questions, such as whether dual targets could lead to improved efficacy, how tight of binding of the drug to the receptor is needed, and, ultimately, what is the efficacious dose in humans and how much increase in muscle volume can be expected at that dose.

The model framework for follistatin and its ligands were adopted from the platform physiologically-based pharmacokinetic model developed by Shah *et al*.[25] Drug in plasma distributes to the interstitial subcompartment of muscle, pituitary, and other tissues via paracellular pores using the convective lymph flow. Based on the general PK/PD model for antibodies that binds to soluble targets,[26] this QSP model assumes that when ligand becomes bound to the drug, the ligand-drug complex takes on the elimination characteristics of the free drug. As being discussed in Davda *et al*.[26] and seen with cases of omalizumab[27] and carlumab,[28] this assumption is plausible to allow the complex to be governed by the same parameters as the drug. The vascular reflection coefficient represents the fraction of drug sieved during the movement of lymph flow through a vessel. In this model, tissue reflection coefficients are assumed to be equal in all tissues, with values depending on its size.[29] The sensitivity analysis showed that the vascular coefficient of muscle tissues is one of the key parameters influencing serum drug and biomarker concentrations, which is consistent with previously published literature regarding vascular reflection coefficient at target tissue.[25]

In the biological process map, myostatin and activin kinetics were built based on baseline levels of these ligands and their binding affinities toward ActRIIB receptor published in literature. Some of key biological parameters are not available or cannot be measured, such as synthesis and cleavage rates of myostatin prepropeptide in muscle and plasma, and synthesis rates of activin prepropeptide in pituitary, muscle, and plasma. Based on the sensitivity analysis, these parameters are less sensitive to plasma exposure of the drug. However, the kinetic rates of ppMyo and myostatin in muscle are critical in predicting the serum profile of free myostatin, which can be expected because these parameters determine the baseline level of the ligand in muscle and plasma. Binding affinity of drug for myostatin ($kon_{drug\text{-}Myo}$ and $koff_{drug\text{-}Myo}$ values) were also found to be important for myostatin disposition prediction. The fitted binding rate constants for adnectin and domagrozumab provide corresponding K_d of 59 pM and 4 pM, accordingly, which are within 2-fold to 3-fold compared with published *in vitro* values of 170 pM[30] and 2.6 pM[31] for these two compounds. Based on this observation, when myostatin data is not available for ACE-031 and FS-EEE-Fc model for accurate estimation of drug-ligand binding rate constants, *in vitro* values were considered reasonable as model inputs.

By fitting the mechanistic model to PK/PD dataset of adnectin and ACE-031, we aimed to evaluate whether the empirical indirect response models of muscle growth and FSH levels are adequate to capture the essence of the underlying pharmacology that relates RO and PD readouts. Due to the limitation of data at the degradation phase of muscle, the estimated PD parameters, especially k_{deg_muscle}, were obtained with moderate to high uncertainty. However, when comparing model prediction of muscle volume increase with observed data of domagrozumab and ACE-031, the overall agreement between prediction and observations in **Table 3** was considered sufficient to qualify the model as fit-for-purpose at this stage and to engender confidence in the model performance. It should be noted that in terms of the model complexity, computational time, and convergence, we took the practical approach to fix the PK parameters and then subsequently fit the PD parameters conditioned on PK information. It was acknowledged that this approach should be applied to models where the PKs are independent of the PD. As a matter of fact, the PKs of many biological agents are highly dependent on the PD response, which often necessitates simultaneous fitting of the data.

Generally, a systems pharmacology model is a complex, dynamic model that consists of both drug-specific and biological system-specific components. With large numbers of model parameters, although some of them can be set to known physiological values, many of them are often unknown, being not measurable, and having experimental variations in different experimental conditions. This poses a certain challenge, particularly when attempting to estimate

unknown parameters via parameter estimation. Hence, to avoid simultaneous large-scale parameter estimation and balance between the number of parameters and goodness of data fitting, analysis of parameter sensitivity, identifiability, and collinearity should be performed to identify key parameters to be fitted during model calibration.[32,33] As demonstrated, local and global SAs can serve as a useful analysis technique for complex system pharmacology models to identify sensitive parameters. In addition, in this study, multivariate parameter identifiability was also performed before fitting by estimating the approximate linear dependence ("collinearity") of parameter sets using the "collin" function in the FME package.[19] Based on the collinearity index chosen to be 20, several combinations of parameter sets (e.g., a set of ka, bioavailability (F), V_{other}, V_{muscle}, $sigma_{o\_V\_drug}$, and k_{syn_ppMyo}, are poorly identifiable and were avoided for fitting simultaneously to the data (results not shown).

Development of an effective drug for muscular dystrophy has been struggling after multiple recent trial failures.[2] These drugs can help build skeletal muscle, but little was known about how much increase in muscle can lead to functional improvement. Determining the level of muscle increase that makes a clinical impact in DMD is critical for the model application and its support in decision making. Based on the recent DMD drug trials, < 7% muscle growth translated into insignificant improvements in patient strength and function over controls. On the flip side, disproportionate muscle enlargement may exaggerate postural instability and joint contractures.[34] More importantly, the major clinical end point of DMD therapeutic interventions is the improvement in the distance walked on the 6MWT. Despite the prominent role of muscle mass in muscular dystrophy, the link between hypertrophy and functionality of the muscle enlargement is not fully understood. Due to limited information, at this point, the causal relationship between extent of muscle volume increase and 6MWT has not been investigated in this model. DMD is a severe disease caused by deletions in the dystrophin gene, leading to destabilizing and gradually degrading muscle. The model could be further expanded to account for the numbers of healthy, damaged, and regenerating muscle cells,[35] which provides more mechanistic insight and understanding, whereas inhibiting myostatin could only produce hypertrophy, but not hyperplasia (more muscle cells), which may not increase strength proportionally.[2]

In conclusion, as demonstrated in this study, using QSP clearly provides quantitative assessments of drug-target interactions between FS-EEE-Fc/myostatin/activin and subsequent PD readouts of muscle volume changes and plasma FSH levels. Despite several clinical trial setbacks, there still remains a high unmet need among patients with DMD and myostatin is still an attractive therapeutic target for muscle atrophy in rare diseases and others, such as sporadic inclusion body myositis and sarcopenia. The presented QSP framework has potential to leverage known biological information of the myostatin signaling pathway and incorporate recent clinical findings to support the ongoing clinical stage drug programs as well as new strategies for targeting myostatin and its family members.

Supporting Information. Supplementary information accompanies this paper on the *CPT: Pharmacometrics & Systems Pharmacology* website (www.psp-journal.com).

Acknowledgments. The authors would like to acknowledge the leadership of the Department of Drug Metabolism and Pharmacokinetics and Quantitative Translational Sciences, Takeda, MA, for supporting this work.

Funding. The study and research was funded by Shire HGT Inc., Lexington, MA, (a member of the Takeda group of companies).

Conflict of Interest. H.Q.N., A.I., and D.E. are employees of Shire HGT Inc. (a Takeda company). D.E. and A.I. own stocks of Takeda. H.R., D.W., and R.N. were employees of Shire HGT Inc. at the time of the study. All authors declared no competing interests for this work.

Author Contributions. H.Q.N. wrote the manuscript. H.Q.N., N.R., H.R., D.W., and Z.Z. designed the research. H.Q.N., P.J., and Z.Z. performed the research. H.Q.N., N.R., H.R., P.J., and Z.Z. analyzed the data. A.I., D.E., and H.R. contributed to new reagents/analytical tools.

1. No authors listed. Railroading at the FDA. *Nat. Med.* **22**, 1193 (2016).
2. Garber, K. No longer going to waste. *Nat. Biotechnol.* **34**, 458 (2016).
3. Lee, S.-J. Quadrupling muscle mass in mice by targeting TGF-ß signaling pathways. *PLoS One* **2**, e789 (2007).
4. Iskenderian, A. *et al.* Myostatin and activin blockade by engineered follistatin results in hypertrophy and improves dystrophic pathology in mdx mouse more than myostatin blockade alone. *Skelet. Muscle* **8**, 34 (2018).
5. Shen, C. *et al.* Protein engineering on human recombinant follistatin: enhancing pharmacokinetic characteristics for therapeutic application. *J. Pharmacol. Exp. Ther.* **366**, 291–302 (2018).
6. Lee, S.-J. & McPherron, A.C. Regulation of myostatin activity and muscle growth. *Proc. Natl. Acad. Sci. USA* **98**, 9306–9311 (2001).
7. Cohn, R.D., Liang, H.-Y., Shetty, R., Abraham, T. & Wagner, K.R. Myostatin does not regulate cardiac hypertrophy or fibrosis. *Neuromuscul. Disord.* **17**, 290–296 (2007).
8. McPherron, A.C., Lawler, A.M. & Lee, S.-J. Regulation of skeletal muscle mass in mice by a new TGF-p superfamily member. *Nature* **387**, 83 (1997).
9. Han, H. & Mitch, W.E. Targeting the myostatin signaling pathway to treat muscle wasting diseases. *Curr. Opin. Support. Palliat. Care* **5**, 334 (2011).
10. Saitoh, M. *et al.* Myostatin inhibitors as pharmacological treatment for muscle wasting and muscular dystrophy. *J. Cachexia Sarcopenia Muscle* **2**, 1–10 (2017).
11. Jones, K.L., De Kretser, D.M., Patella, S. & Phillips, D.J. Activin A and follistatin in systemic inflammation. *Mol. Cell Endocrinol.* **225**, 119–125 (2004).
12. Latres, E. *et al.* Activin A more prominently regulates muscle mass in primates than does GDF8. *Nat. Commun.* **8**, 15153 (2017).
13. Chen, J.L. *et al.* Development of novel activin-targeted therapeutics. *Mol. Ther.* **23**, 434–444 (2015).
14. Lee, S.-J. *et al.* Regulation of muscle mass by follistatin and activins. *Mol. Endocrinol.* **24**, 1998–2008 (2010).
15. Gilson, H. *et al.* Follistatin induces muscle hypertrophy through satellite cell proliferation and inhibition of both myostatin and activin. *Am. J. Physiol. Endocrinol. Metab.* **297**, E157–E164 (2009).
16. Jacobsen, L.BMS-986089: an antimyostatin adnectin targeting Duchenne muscular dystrophy. Presented at: Parent Project Muscular Dystrophy Connect Conference, June 26–29, 2016, Orlando, FL.
17. Attie, K.M. *et al.* A single ascending-dose study of muscle regulator ACE-031 in healthy volunteers. *Muscle Nerve* **47**, 416–423 (2013).
18. Bhattacharya, I. *et al.* Safety, tolerability, pharmacokinetics, and pharmacodynamics of domagrozumab (PF-06252616), an antimyostatin monoclonal antibody, in healthy subjects. *Clin. Pharm. Drug Dev.* **7**, 484–497 (2018).
19. Soetaert, K. & Petzoldt, T. Inverse modelling, sensitivity and Monte Carlo analysis in R using package FME. *J. Stat. Softw.* **33**, 1–28 (2010).
20. Oitate, M. *et al.* Prediction of human pharmacokinetics of therapeutic monoclonal antibodies from simple allometry of monkey data. *Drug Metab. Pharmacokinet.* **26**, 423–430 (2011).
21. Wagner, K. *et al.* A randomized, placebo-controlled, double-blind, phase 1b/2 study of the novel antimyostatin adnectin RG6206 (BMS-986089) in ambulatory boys with Duchenne muscular dystrophy (P5.431). *Neurology* **90**(15 suppl), P5.431 (2018).

22. Campbell, C. *et al.* Myostatin inhibitor ACE-031 treatment of ambulatory boys with Duchenne muscular dystrophy: results of a randomized, placebo-controlled clinical trial. *Muscle Nerve* **55**, 458–464 (2017).
23. Rooks, D.S. *et al.* Effect of bimagrumab on thigh muscle volume and composition in men with casting-induced atrophy. *J. Cachexia Sarcopenia Muscle* **8**, 727–734 (2017).
24. Amato, A.A. *et al.* Treatment of sporadic inclusion body myositis with bimagrumab. *Neurology* **83**, 2239–2246 (2014).
25. Shah, D.K. & Betts, A.M. Towards a platform PBPK model to characterize the plasma and tissue disposition of monoclonal antibodies in preclinical species and human. *J. Pharmacokinet. Phar.* **39**, 67–86 (2012).
26. Davda, J.P. & Hansen, R.J. Properties of a general PK/PD model of antibody-ligand interactions for therapeutic antibodies that bind to soluble endogenous targets. *MAbs* **2**, 576–588 (2010).
27. Hayashi, N., Tsukamoto, Y., Sallas, W.M. & Lowe, P.J. A mechanism-based binding model for the population pharmacokinetics and pharmacodynamics of omalizumab. *Brit. J. Clin. Pharmacol.* **63**, 548–561 (2007).
28. Fetterly, G.J. *et al.* Utilizing pharmacokinetics/pharmacodynamics modeling to simultaneously examine free CCL2, total CCL2 and carlumab (CNTO 888) concentration time data. *J. Clin. Pharmacol.* **53**, 1020–1027 (2013).
29. Li, Z. & Shah, D.K. Two-pore physiologically based pharmacokinetic model with de novo derived parameters for predicting plasma PK of different size protein therapeutics. *J. Pharmacokinet. Phar.* **46**, 305–318 (2019).
30. Madireddi, M. *et al.* BMS-986089 is a high affinity anti-myostatin adnectin that increases muscle volume in three preclinical species. *Neuromuscul. Disord.* **26**, S94–S95 (2016).
31. Andre, M.S. *et al.* A mouse anti-myostatin antibody increases muscle mass and improves muscle strength and contractility in the mdx mouse model of Duchenne muscular dystrophy and its humanized equivalent, domagrozumab (PF-06252616), increases muscle volume in cynomolgus monkeys. *Skelet. Muscle* **7**, 25 (2017).
32. Andre, M.S. *et al.* QSP Toolbox: computational implementation of integrated workflow components for deploying multi-scale mechanistic models. *AAPS J.* **19**, 1002–1016 (2017).
33. Zhang, X.Y., Trame, M., Lesko, L. & Schmidt, S. Sobol sensitivity analysis: a tool to guide the development and evaluation of systems pharmacology models. *CPT Pharmacometrics Syst. Pharmacol.* **4**, 69–79 (2015).
34. Kornegay, J.N. *et al.* The paradox of muscle hypertrophy in muscular dystrophy. *Phys. Med. Rehabil. Clinic* **23**, 149–172 (2012).
35. Cameron, A.N., Houston, M.T. & Gutierrez, J.B.A review of mathematical models for muscular dystrophy: a systems biology approach. arXiv preprint arXiv:161003521. (2016).
36. Tries, R.S. *et al.* GDF-8 propeptide binds to GDF-8 and antagonizes biological activity by inhibiting GDF-8 receptor binding. *Growth Factors* **18**, 251–259 (2001).
37. Wakefield, L. *et al.* Regulation of transforming growth factor-β subtypes by members of the steroid hormone superfamily. *J. Cell Sci.* **1990**, 139–148 (1990).
38. Sako, D. *et al.* Characterization of the ligand binding functionality of the extracellular domain of activin receptor type IIb. *J. Biol. Chem.* **M110**, 114959 (2010).
39. Johnson, K.E. *et al.* Biological activity and in vivo half-life of pro-activin A in male rats. *Mol. Cell Endocrinol.* **422**, 84–92 (2016).
40. Richter, W.F. & Jacobsen, B. Subcutaneous absorption of biotherapeutics: knowns and unknowns. *Drug Metab. Dispos.* **42**, 1881–1889 (2014).
41. Bhattacharya, I., Manukyan, Z., Chan, P., Heatherington, A. & Harnisch, L. Application of quantitative pharmacology approaches in bridging pharmacokinetics and pharmacodynamics of domagrozumab from adult healthy subjects to pediatric patients with Duchenne muscular disease. *J. Clin. Pharmacol.* **58**, 314–326 (2018).
42. Landry, J., Ke, Y., Yu, G.-L. & Zhu, X. Measuring affinity constants of 1450 monoclonal antibodies to peptide targets with a microarray-based label-free assay platform. *J. Immunol. Methods* **417**, 86–96 (2015).